JOURNAL OF AGRICULTURAL AND FOOD CHEMISTRY

Article

pubs.acs.org/JAFC

Renal Injury and Nrf2 Modulation in Mouse Kidney Following Chronic Exposure to TiO_2 Nanoparticles

Suxin Gui,[†,∥] Bingyan Li,[†,∥] Xiaoyang Zhao,[†,∥] Lei Sheng,[†,∥] Jie Hong,[†,∥] Xiaohong Yu,[†] Xuezi Sang,[†] Qingqing Sun,[†] Yuguan Ze,[†] Ling Wang,[†] and Fashui Hong*[,†,§,#]

[†]Medical College of Soochow University, Suzhou 215123, China

[§]Jiangsu Province Key Laboratory of Stem Cell Research, Soochow University, 708 Renmin Road, Suzhou 215007, China

[#]Cultivation Base of State Key Laboratory of Stem Cell and Biomaterials built together by Ministry of Science and Technology and Jiangsu Province, Suzhou 215007, China

ABSTRACT: TiO_2 nanoparticles (NPs) are used in the food industry but have potential toxic effects in humans and animals. TiO_2 NPs impair renal function and cause oxidative stress and renal inflammation in mice, associated with inhibition of nuclear factor erythroid-2-related factor 2 (Nrf2), which regulates genes encoding many antioxidants and detoxifying enzymes. This study determined whether TiO_2 NPs activated the Nrf2 signaling pathway. Mice exhibited accumulation of reactive oxygen species and peroxidation of lipid, protein, and DNA in the kidney, coupled with renal dysfunction, glutathione depletion, inflammatory cell infiltration, fatty degeneration, and apoptosis. These were associated with increased expression of NOX4, cyclooxygenase-2, and nuclear factor-κB. Oxidative stress and inflammation were accompanied by decreased expression of Nrf2 and down-regulation of its target gene products including heme oxygenase 1, glutamate−cysteine ligase catalytic subunit, and glutathione *S*-transferase. Chronic TiO_2 NP exposure is associated with suppression of Nrf2, which contributes to the pathogenesis of oxidative stress and inflammation.

KEYWORDS: *titanium dioxide nanoparticles, kidney, oxidative stress, inflammation, Nrf2 pathway*

INTRODUCTION

TiO_2 nanoparticles (NPs) are frequently used in vitamin manufacturing. According to U.S. federal regulations, the quantity of TiO_2 (non-NPs) should not exceed 1% by weight of the food. Currently, TiO_2 NPs are used in the food industry, dietary supplements, and crop production.[1−3] In addition, TiO_2 NPs are applied widely in other areas such as medicine, consumer products, paints and surface coatings, and environmental decontamination of air, soil, and water.[4−9] Although TiO_2 is considered to be a safe material, concerns have been raised about its potential adverse health effects in humans and animals.[10,11] As a result of its toxic potential, TiO_2 has been classified by the International Agency for Research on Cancer as "possibly carcinogenic to humans" by inhalation.[12] A major route of human exposure to TiO_2 NPs is through food intake and its use as a pharmaceutical additive, where TiO_2 NPs are used widely as food-coloring agents.[13]

The photocatalytic properties of TiO_2 NPs cause various toxic effects in the lungs,[14−17] gills,[18] liver,[19−26] spleen,[27−30] brain,[31−38] reproductive system,[39,40] and heart[41] in animals. Specifically, exposure to TiO_2 NPs can cause renal injuries. For instance, TiO_2 NPs accumulate in the kidneys of rainbow trout;[42] increase blood urea nitrogen and creatinine levels in rats, resulting in renal tubular damage,[19] and cause glomerular dilatation in mice.[43] Our previous studies also suggested that TiO_2 NP exposure led to renal injury and dysfunction.[44−47] Toxicity is exerted through overproduction of reactive oxygen species (ROS) and altered expression of inflammation-related cytokines in mice. However, the molecular mechanism of TiO_2 NP-induced renal oxidative damage is still not well understood.

Excess production of ROS causes tissue injury and dysfunction by impairing structural and functional molecules and by stimulating redox-sensitive transcription factors and signal transduction pathways. These events lead to necrosis, apoptosis, and inflammation. Redox systems including antioxidant enzymes and phase II detoxifying and antioxidant agents provide protection against ROS-induced tissue injury. Nuclear factor erythroid-2-related factor 2 (Nrf2) plays an important role in basal activity and coordinated induction of genes encoding numerous antioxidant and phase II detoxifying enzymes and related proteins.[48] To explore the molecular mechanism of TiO_2 NP-induced oxidative stress in mouse kidney, it is necessary to focus on the oxidative stress-responding Nrf2/antioxidant responsive elements (AREs) pathway of nephrotoxicity. Nrf2 can be evaluated as target transcription factors of TiO_2 NP-induced toxicity. When activated by oxidative stress, Nrf2 breaks free from Kelch-like ECH-associated protein 1 (Keap1) and translocates into the nucleus, where it binds to an antioxidant response factor, a cis-acting enhancer sequence that mediates the transcriptional activation of genes in response to oxidative stress, including heme oxygenase (HO)-1[49] and glutamate−cysteine ligase catalytic subunit (GCLC).[50] They have antioxidant capacity and act as potent anti-inflammatory proteins whenever oxidative injury takes place.[51] Rapid induction of HO-1 follows

Received: May 31, 2013
Revised: August 14, 2013
Accepted: August 22, 2013
Published: August 22, 2013

 © 2013 American Chemical Society

various stresses.[52−54] Previous studies have suggested protective roles of HO-1 and GCLC in various inflammatory and apoptotic conditions.[55−61] Progression of renal disease in mice is largely driven by inflammation and oxidative stress under conditions of TiO_2 NP-induced nephrotoxicity.[43−47] Oxidative stress and inflammation are inseparably linked, and they form a vicious cycle in which oxidative stress provokes inflammation by several mechanisms, including activation of nuclear factor (NF)-κB, which leads to the activation and recruitment of immune cells. Inflammation, in turn, provokes oxidative stress via production of reactive oxygen, nitrogen, and halogen species by activated leukocytes and resident cells. Glutathione *S*-transferase (GST) is a major cellular detoxification enzyme. This enzyme catalyzes the conjugation of various electrophiles with reduced glutathione, which plays an important role in biotransformation of xenobiotic and endogenous toxic compounds. The role of GST is considered to be an important mechanism in resistance to toxicants of animals.[62,63] In addition, GST has non-selenium-dependent glutathione peroxidase activity and can remove highly reactive electrophilic components, such as lipid hydroperoxide.[64] Due to its detoxification function and antioxidative activity, GST can be specifically induced by xenobiotic toxic compounds and might contribute to improved toxicant tolerance. Induction of GST activity was found in animal exposure to xenobiotic compounds.[65] Thus, GST is often used as an oxidative stress biomarker. Together, these events promote tissue damage by inflicting apoptosis, necrosis, and fibrosis. We hypothesized that TiO_2 NP-induced renal inflammation and oxidative damage may be associated with the Nrf2 pathway in mouse kidney.

In the present study, mice were continuously exposed to 2.5, 5, or 10 mg/kg TiO_2 NPs administered by intragastric instillation for 6 consecutive months. Oxidative stress and alterations in inflammatory cytokine expression in mouse kidney were investigated to determine the mechanisms of Nrf2−Keap1 activation in renal inflammation and oxidative stress caused by TiO_2 NP exposure.

MATERIALS AND METHODS

Chemicals and Preparation. Anatase TiO_2 NPs were prepared via controlled hydrolysis of titanium tetrabutoxide, as described previously.[35,66] X-ray diffraction (XRD) measurements showed that TiO_2 NPs exhibited a 101 peak of anatase. The average particle size of powdered TiO_2 NPs suspended in 0.5% w/v hydroxypropylmethylcellulose (HPMC) K4M solvent after 24 h (5 mg/mL) of incubation ranged from 5 to 6 nm, and the surface area was 174.8 m^2/g. The mean hydrodynamic diameter of TiO_2 NPs in HPMC solvent (5 mg/mL) ranged from 208 to 330 nm (mainly 294 nm), and the ζ potential after 24 h of incubation was 9.28 mV.

Animals and Treatment. One hundred and sixty CD-1 (ICR) male mice (20 ± 2 g body weight) were purchased from the Animal Center of Soochow University (China). All mice were housed in stainless steel cages in a ventilated animal room. Room temperature of the housing facility was maintained at 24 ± 2 °C with a relative humidity of 60 ± 10% and a 12 h light/dark cycle. Distilled water and sterilized food were available for mice ad libitum. Prior to dosing, the mice were acclimated to this environment for 5 days. All procedures used in animal experiments conformed to the U.S. National Institutes of Health *Guide for the Care and Use of Laboratory Animals*.

TiO_2 NP powder was dispersed onto the surface of 0.5% w/v HPMC, and the suspension containing TiO_2 NPs was treated ultrasonically for 30 min and mechanically vibrated for 5 min. The mice were randomly divided into four groups (n = 40 each), including a control group treated with 0.5% w/v HPMC and three experimental groups treated with 2.5, 5, and 10 mg/kg TiO_2 NPs. For dose selection, we consulted a report of the World Health Organization from 1969. According to the report, the LD_{50} of TiO_2 for rats is >12 g/kg body weight after oral administration. In addition, the quantity of TiO_2 NPs does not exceed 1% by weight of the food according to U.S. federal regulations. In the present study, we selected 2.5, 5, and 10 mg/kg TiO_2 NPs, which were given to mice by intragastric administration every day. They were equal to about 0.15−0.7 g of TiO_2 NPs for humans with 60−70 kg body weight with such exposure, which are relatively safe doses. The mice were weighed, the volume of TiO_2 NP suspensions was calculated for each mouse, and the fresh TiO_2 NP suspensions were administered to the mice by intragastric administration every day for 6 months. Any symptoms, growth state, eating, drinking, and activity or mortality, were observed and recorded carefully daily during the 6 months.

Kidney Indices. After 6 months, mice were weighed and then sacrificed after ether anesthesia. Blood samples were collected from the eye vein by rapidly removing the eyeball, and serum was collected by centrifuging the blood samples at 1200*g* for 10 min. The kidneys of all animals were quickly removed and placed on ice. After weighing the body and kidneys, the kidney indices were calculated as the ratio of kidney (wet weight, mg) to body weight (g).

Titanium Content Analysis. The frozen renal tissues (n = 5 each) were thawed and approximately 0.3 g samples were weighed, digested, and analyzed for titanium content. Prior to elemental analysis, the renal tissues were digested overnight with nitric acid (ultrapure grade), combined with 0.5 mL of H_2O_2, and incubated at 160 °C in high-pressure reaction containers in an oven until the samples were completely digested. The solutions were incubated at 120 °C to remove any remaining nitric acid until the solutions were clear. Finally, the remaining solutions were diluted to 3 mL with 2% nitric acid. Inductively coupled plasma−mass spectrometry (ICP-MS; Thermo Elemental X7; Thermo Electron Co., Waltham, MA, USA) was used to determine the titanium concentration in the samples. Indium (20 ng/mL) was chosen as an internal standard element. Elemental titanium (isotopes ^{48}Ti or ^{49}Ti) was quantified using ICP-MS against titanium standards, which also contained the internal standard.

Biochemical Analysis of Kidney Functions. Kidney functions (n = 10 each) were determined by uric acid (UA), blood urea nitrogen (BUN), creatinine (CR), and urinary protein excretion. All biochemical assays were performed using a clinical automatic chemistry analyzer (type 7170A, Hitachi, Japan).

Histopathological Examination of Kidney. All histopathological examinations were performed using standard laboratory procedures. Five sets of kidney tissues from mice were embedded in paraffin blocks, sliced to 5 μm thickness, and placed on separate glass slides (five slices from each kidney). After hematoxylin−eosin staining, the sections were evaluated by a histopathologist unaware of the treatments, using an optical microscope (U-III Multipoint Sensor System; Nikon, Tokyo, Japan).

Oxidative Stress Assay. Superoxide ion ($O_2^{\bullet-}$) in the kidney tissues (n = 5 each) was measured by monitoring the reduction of 3′-{1-[(phenylamino)carbonyl]-3,4-tetrazolium}bis(4-methoxy-6-nitro)-benzenesulfonic acid hydrate (XTT) in the presence of $O_2^{\bullet-}$, as described by Oliveira et al.[67] Correction was made for the background absorbance in the presence of 50 U of superoxide dismutase (SOD). The production rate of $O_2^{\bullet-}$ was calculated using an extinction coefficient of $2.16 \times 10^4\ M^{-1}\ cm^{-1}$.

The detection of H_2O_2 in the kidney tissues (n = 5 each) was carried out by the xylenol orange assay.[68] After preincubation with pregnanediol/mercurials and/or quercetin/catalase (30 min at 25 °C), the reaction medium was centrifuged at 17500*g* for 10 min at 4 °C, and the supernatant was incubated for 30 min in a reaction medium containing 250 mM perchloric acid, 2.5 mM ammonium iron(II) sulfate hexahydrate, and 1 mM xylenol orange. H_2O_2 levels were determined at 560 nm using an H_2O_2 curve as standard.

Lipid peroxidation of kidneys (n = 5 each) was determined as the concentration of malondialdehyde (MDA) generated by the thiobarbituric acid (TBA) reaction as described by Buege and Aust.[69] Protein oxidation of kidneys was investigated according to the method of Fagan et al. by determining the protein carbonyl (PC)

Table 1. Real-Time PCR Primer Pairs: PCR Primers Used in the Gene Expression Analysis

gene name	description	primer sequence	primer size (bp)
Refer-actin	mactin-F	5′-GAGACCTTCAACACCCCAGC-3′	
	mactin-R	5′-ATGTCACGCACGATTTCCC-3′	263
NF-κB	mnf-κb-F	5′-GGTGGAGGCATGTTCGGTA-3′	
	mnf-κb-R	5′-TGACCCCTGCGTTGGATT-3′	142
IκB	miκb-F	5′-GGTGCAGGAGTGTTGGTGG-3′	
	miκb-R	5′-TGGCTGGTGTCTGGGGTAC-3′	173
COX-2	mcox-2-F	5′-CTGAGTGGGGTGATGAGCAA-3′	
	mcox-2-R	5′-AGGCAATGCGGTTCTGATACT-3′	174
NOX4	mnox4-F	5′-CCGGCGTGATTACCAAGGTTGTCAT-3′	
	mnox4-R	5′-ATGACAACCTTGGTAATCACGTTTTTG-3′	259
Nrf2	mNrf2-F	5′-CTTCCATTTACGGAGACCCACC-3′	
	mNrf2-R	5′-GGATTCACGCATAGGAGCACTG-3′	176
Keap1	mkeap-1-F	5′-GATCGGCTGCACTGA ACTG-3′	
	mkeap-1-R	5′-GGACTCGCAGCGTACGTT-3′	106
HO-1	mHO-1-F	5′-GACAGAAGAGGCTAAGACCGC-3′	
	mHO-1-R	5′-TGGAGGAGCGGTGTCTGG-3′	213
GCLC	mGCLC -F	5′-ATGTGGACACCCGATGCAGTATT-3′	
	mGCLC -R	5′- GTCTTGCTTGTAGTCAGGATGGTTT-3′	200
GST	mGST -F	5′-CCGCTCTTTGGGGCTTTAT-3′	
	mGST -R	5′-GGTTCTGGGACAGCAGGGT-3′	191

content.[70] Kidney DNA damage was determined as the concentration of 8-hydroxydeoxyguanosine (8-OHdG) using an ELISA kit (Japan Institute for the Control of Aging, Haruoka, Japan).

Assay of Glutathione. To determine reduced glutathione (GSH) and oxidized glutathione (GSSG) levels, the kidneys (n = 5 each) were homogenized as described above. GSH and GSSG contents were estimated using the method of Hissin and Hilf.[71] The reaction mixture contained 100 mL of supernatant, 100 mL of *O*-phthaldehyde (1 mg/mL), and 1.8 mL of phosphate buffer (0.1 M sodium phosphate, 0.005 M EDTA, pH 8). Fluorometry was performed using an F-4500 fluorometer (Hitachi, Japan) with excitation at 350 nm and emission at 420 nm.

Assay of Cytokine Expression. The levels of mRNA expression of *NF-κB*, *IκB*, *Nrf2*, *Keap1*, *COX-2*, *NOX4*, *HO-1*, *GCLC*, and *GST* in the kidneys (n = 5 each) were determined using real-time quantitative (q)RT-PCR, as described previously.[72−74] Synthesized cDNA was generated by qRT-PCR with primers designed with Primer Express Software (Applied Biosystems, Foster City, CA, USA) according to the manufacturer's guidelines, and the sequences are listed in Table 1. To determine NF-κB, IκB, Nrf2, Keap1, cyclo-oxygenase (COX)-2, NOX4, HO-1, GCLC, and GST levels in mouse kidney tissues, ELISA was performed using commercial kits that were selective for each respective protein (R&D Systems, Minneapolis, MN, USA), following the manufacturer's instructions. The absorbance was measured on a microplate reader at 450 nm (Varioskan Flash; Thermo Electron, Finland), and the concentrations of NF-κB, IκB, Nrf2, Keap1, COX-2, NOX4, HO-1, GCLC, and GST were calculated from a standard curve for each sample.

Statistical Analysis. All results are expressed as means ± SEM. Significant differences were examined by unpaired Student's test using SPSS version 19 software (Chicago, IL, USA). $P < 0.05$ was considered statistically significant.

RESULTS

Body Weight, Kidney Indices, and Titanium Accumulation. Figure 1 shows the net increase in body weight and kidney indices caused by TiO_2 NP exposure. TiO_2 NP exposure resulted in significant reductions in body weight and increases in kidney indices as compared with the controls ($P < 0.05$). Furthermore, there was significant titanium accumulation with increased TiO_2 NP dose (Figure 2, $P < 0.01$). The increased

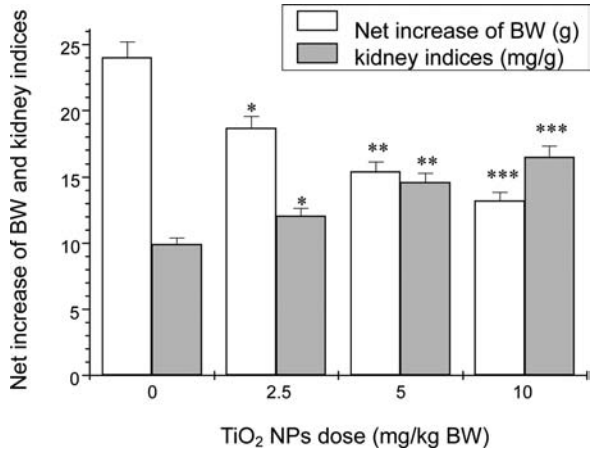

Figure 1. Body weight and kidney indices of male mice after intragastric administration of TiO_2 NPs for 6 consecutive months. * $P < 0.05$, ** $P < 0.01$, and *** $P < 0.001$. Values represent means ± SEM (n = 40).

dx.doi.org/10.1021/jf402387e | J. Agric. Food Chem. 2013, 61, 8959−8968

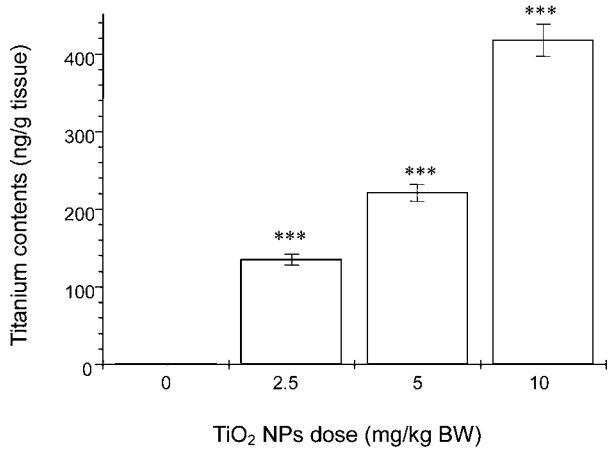

Figure 2. Titanium accumulation in mouse kidneys after intragastric administration of TiO_2 NPs for 6 consecutive months. *** $P < 0.001$. Values represent means ± SEM ($n = 5$).

kidney indices caused by TiO_2 NP exposure may be related to kidney dysfunction and tissue injury, which were confirmed by the biochemical assays and histopathological observations of mouse kidneys.

Oxidative Stress Analysis. The effects of TiO_2 NPs on the production of $O_2^{\bullet-}$ and H_2O_2 in mouse kidney tissues are shown in Figure 3. With increased TiO_2 NP dose, the rate of

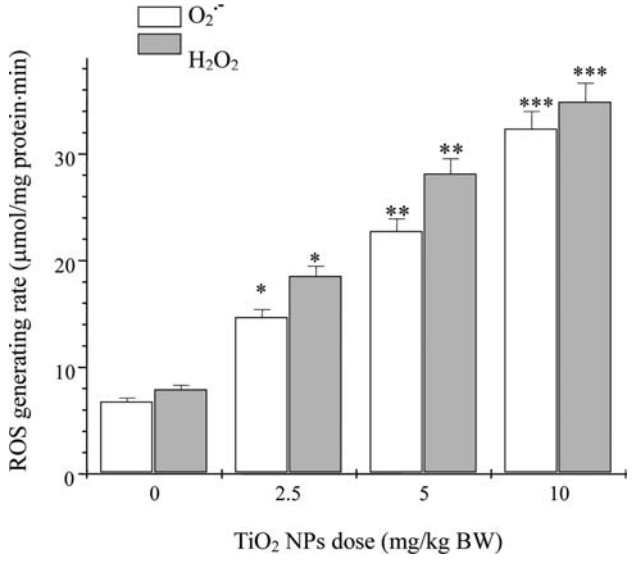

Figure 3. ROS accumulation in mouse kidneys after intragastric administration of TiO_2 NPs for 6 consecutive months. * $P < 0.05$, ** $P < 0.01$, *** $P < 0.001$. Values represent means ± SEM ($n = 5$).

ROS generation in the mice exposed to TiO_2 NPs was significantly elevated ($P < 0.05$), suggesting that chronic exposure to TiO_2 NPs accelerated ROS production in the kidney tissues. To confirm the effects of TiO_2 NPs on ROS generation in mouse kidney, the levels of MDA, PC, and 8-OHdG were examined. As shown in Figure 4, levels of MDA, PC, and 8-OHdG in the kidney tissues from the TiO_2 NP-exposed groups were markedly elevated ($P < 0.05$), suggesting that TiO_2 NP-induced ROS accumulation led to lipid, protein, and DNA peroxidation in the kidneys.

Histopathological Evaluation. The histological changes in the kidney specimens are shown in Figure 5. Unexposed

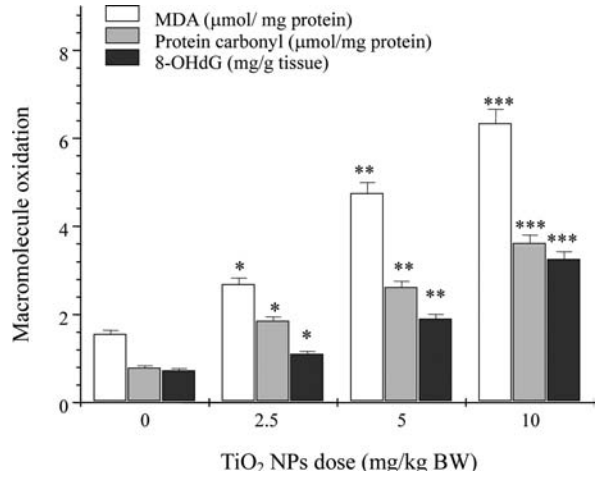

Figure 4. Peroxide levels of lipid, protein, and DNA in mouse kidneys after intragastric administration of TiO_2 NPs for 6 consecutive months. * $P < 0.05$, ** $P < 0.01$, and *** $P < 0.001$. Values represent means ± SEM ($n = 5$).

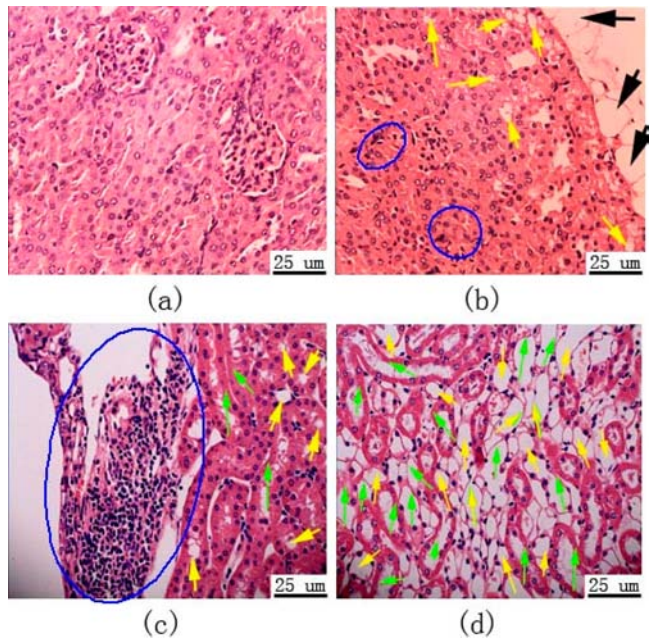

Figure 5. Histopathological observation of kidneys after intragastric administration of TiO_2 NPs for 6 consecutive months ($n = 5$): (a) control group (unexposed mice) showed intact glomeruli; (b) 2.5 mg/kg TiO_2 NPs group presented with slight inflammatory cell infiltration (blue cycle), fatty degeneration (yellow arrows), and degeneration of superficial adipocytes (black arrows); (c) 5 mg/kg TiO_2 NPs group presented with inflammatory cell infiltration (blue cycle), fatty degeneration (yellow arrows), and apoptosis of renal tubules (green arrows); (d) 10 mg/kg TiO_2 NPs group presented with severe fatty degeneration (yellow arrows) and apoptosis of renal tubules (green arrows).

kidney samples exhibited normal architecture (Figure 5a), whereas those from five mice of each group exposed to increasing TiO_2 NP concentrations exhibited severe pathological changes, including infiltration of inflammatory cells, fatty degeneration, and apoptosis (Figure 5b–d). The results suggested that chronic exposure to TiO_2 NPs resulted in significant pathological changes in the kidneys, which were related to oxidative stress.

dx.doi.org/10.1021/jf402387e | J. Agric. Food Chem. 2013, 61, 8959–8968

Kidney Function. The changes in the serum biochemical parameters induced by TiO_2 NP exposure are presented in Figure 6. With increased TiO_2 NP dose, CR and protein/CR ratio increased, whereas the UA and BUN were decreased gradually ($P < 0.05$ or 0.01), respectively.

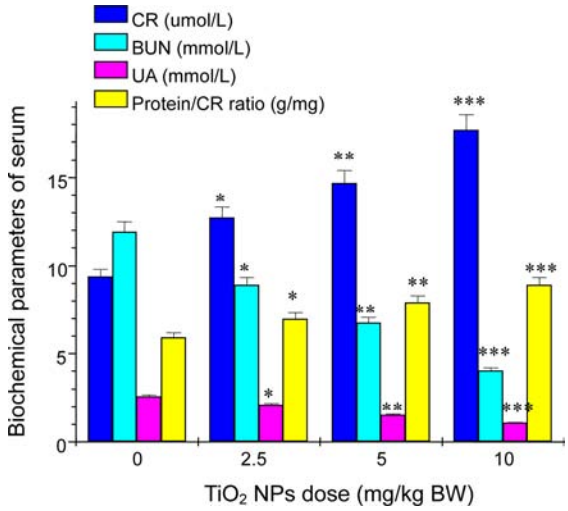

Figure 6. Alterations in serum biochemical parameters of mice after intragastric administration of TiO_2 NPs for 6 consecutive months. * $P < 0.05$, ** $P < 0.01$, and *** $P < 0.001$. Values represent means ± SEM ($n = 10$).

Nrf2/Keap1 Pathway. Mice with TiO_2 NP-induced nephropathy presented with a significant, dose-dependent reduction in nuclear Nrf2 expression and a dose-dependent marked increase in Keap1 expression in kidney tissue (Figure 7) ($P < 0.05$). These were associated with marked down-regulation of the measured Nrf2 target gene products, including GST, HO-1, and GCLC in mouse kidney under conditions of TiO_2 NP-induced nephropathy ($P < 0.05$). These findings point to the impaired activation of the Nrf2 pathway in mice following exposure to TiO_2 NPs.

Total GSH Level. To explore further the effects of TiO_2 NPs on GCLC and GST expression, the total GSH content (GSH + GSSG) in the kidneys was determined (Figure 8). As the dose of TiO_2 NPs increased, there was a significant reduction in total GSH level in the kidneys ($P < 0.05$). These results suggested that decreased GSH level caused by TiO_2 NPs exposure was associated with decreased GCLC and GST expression.

Oxidative and Inflammatory Pathways. Figure 9 shows the effects of TiO_2 NPs on NF-κB, IκB, NADPH oxidase (NOX), and COX-2 expressions in mouse kidney. With increased TiO_2 NP doses, there was a significant increase in NF-κB, and a marked reduction in IκB expression in the kidney tissue ($P < 0.05$). These were accompanied by marked increases in NOX4 and COX-2 expression in mouse kidneys following exposure to TiO_2 NPs.

DISCUSSION

The results of the present study indicate that intragastric administration of 2.5, 5, and 10 mg/kg of TiO_2 NPs for 6 consecutive months induced body weight reduction and increased kidney indices and titanium accumulation. This led to severe oxidative stress, marked by significant production of $O_2^{\cdot-}$ and H_2O_2, and peroxidation of lipids, proteins, and DNA,

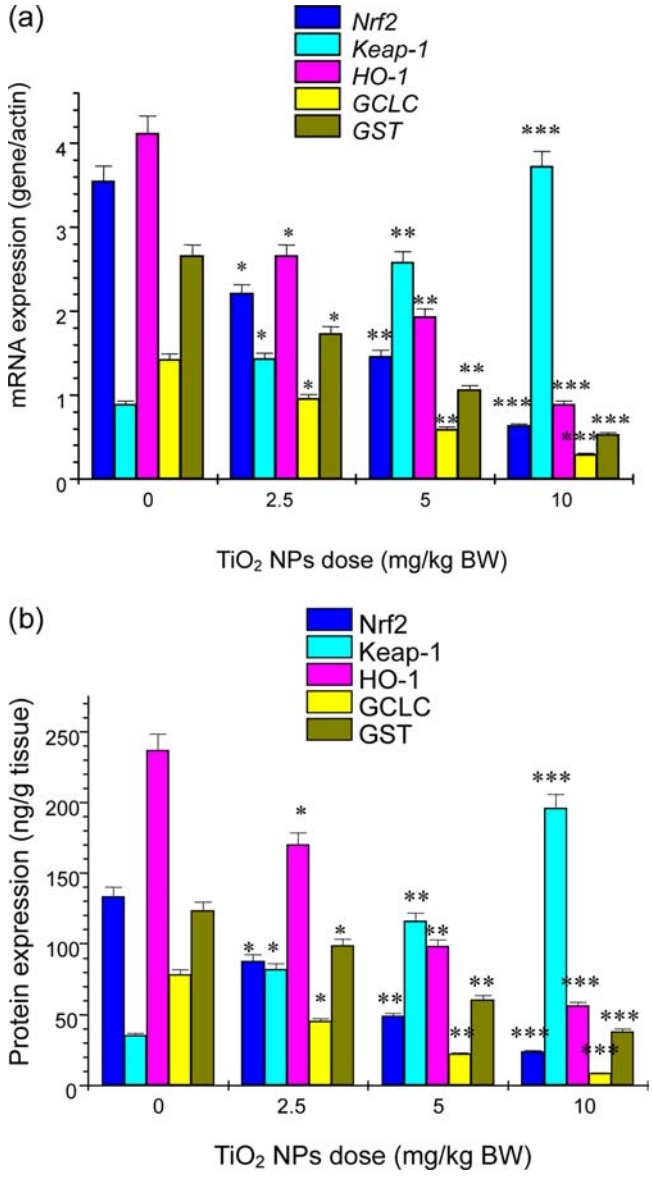

Figure 7. Alterations of Nrf2, Keap-1, HO-1, GCLC, and GST expression in mouse kidneys after intragastric administration of TiO_2 NPs for 6 consecutive months. * $P < 0.05$, ** $P < 0.01$, and *** $P < 0.001$. Values represent means ± SEM ($n = 5$).

coupled with inflammatory response, fatty degeneration, and apoptosis in the renal tubules. Eating, drinking, and activity of mice following exposure to TiO_2 NPs were lower than in the untreated controls. Decreased body weight of mice caused by TiO_2 NPs might have been due to loss of appetite and decreased appetite to ROS accumulation and decreased antioxidant activities following exposure to TiO_2 NPs. Recent studies have confirmed a pivotal role of ROS in food intake and energy homeostasis regulation in the hypothalamus. For example, in response to an acute overload of nutrients, elevation of ROS concentration was sufficient to reduce food intake.[75] It has also been suggested that the central and peripheral administration of glucose can reduce food intake due to enhanced ROS levels in the hypothalamus.[76,77] Our findings suggested that with increased TiO_2 NP doses, body weight of mice was significantly decreased, whereas ROS production was greatly elevated in the kidneys. Scown et al. have suggested that TiO_2 NPs accumulate in the kidneys, but have minimal effects

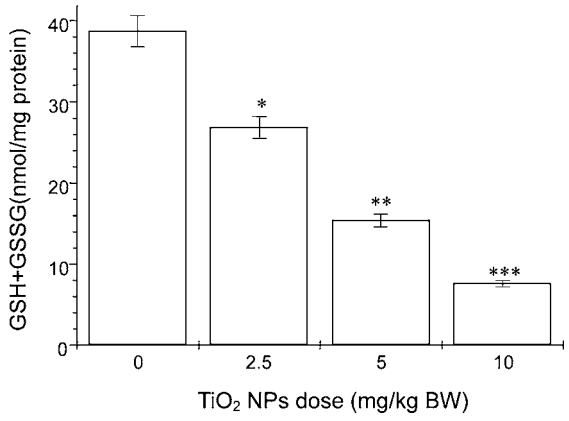

Figure 8. Total GSH levels in mouse kidneys after intragastric administration of TiO_2 NPs for 6 consecutive months. $* P < 0.05$, $** P < 0.01$, and $*** P < 0.001$. Values represent means ± SEM ($n = 5$).

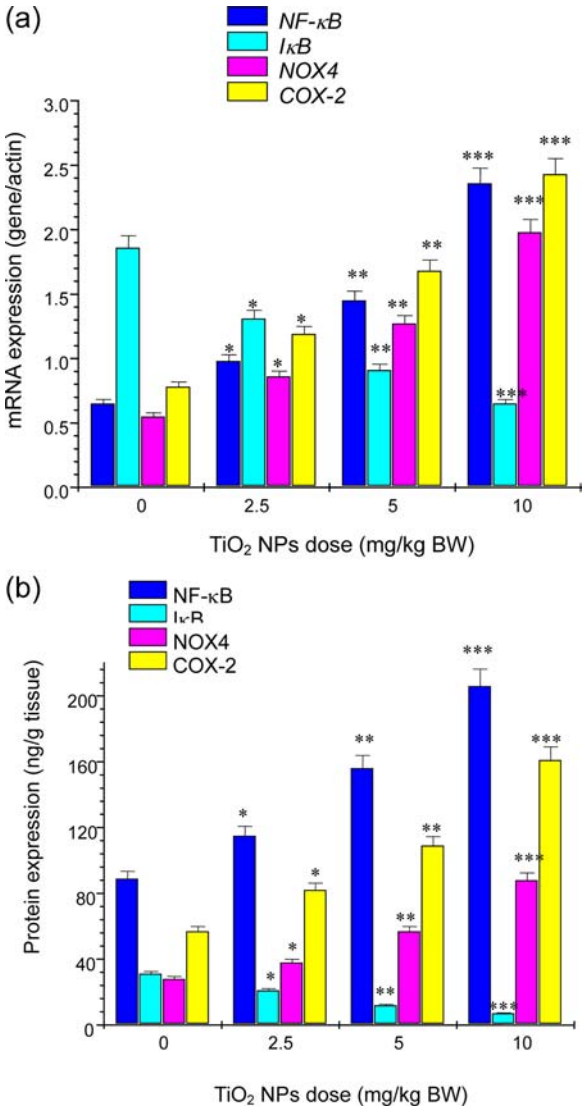

Figure 9. Alterations of NF-κB, IκB, NOX, and COX-2 expression in mouse kidneys after intragastric administration of TiO_2 NPs for 6 consecutive months. $* P < 0.05$, $** P < 0.01$, and $*** P < 0.001$. Values represent means ± SEM ($n = 5$).

on renal function in rainbow trout.[42] In contrast, Wang et al. found that TiO_2 NP exposure resulted in higher BUN and serum CR levels and the renal tubules were filled with proteinic liquids in mice, but they did not observe obvious differences in the kidney indices of the female mice.[19] Chen et al. also observed glomerular dilatation and proteinic liquids in the renal tubules, but no kidney dysfunction was observed in mice exposed to TiO_2 NPs.[43] Our previous studies have indicated that TiO_2 NP exposure causes renal dysfunction and increases in kidney indices.[44,46,47] Recently, Sardari et al. observed glomerular cell necrosis and protein sediment in the Bowman capsules and proximal tubules in rats exposed to silver NPs.[78] Our data also suggest that chronic exposure to TiO_2 NPs resulted in significant increases in CR and proteinuria and reductions in UA and BUN. Serum BUN is excreted through the glomeruli. A range of changes in the urinary excretion of taurine and CR may be induced by nephrotoxins. When the kidneys are injured, CR and protein increase and serum UA and BUN decrease. Our previous studies have demonstrated that exposure to TiO_2 NPs leads to adverse responses such as oxidative damage and inflammation in mouse kidneys, but the molecular targets of oxidative damage caused by TiO_2 NPs remain unclear.[44−47] Inflammation and apoptosis in renal tubules following exposure to TiO_2 NPs are due to excess ROS production and modulation of the Nrf2 pathway.

As shown in the present study, TiO_2 NP-induced accumulation of ROS such as $O_2^{\dot{\bullet}-}$ and H_2O_2 in mouse kidneys resulted in oxidative damage of biological macromolecules, including lipid, protein, and DNA peroxidation. This oxidative damage happened before TiO_2 NP-induced renal inflammation or apoptosis became evident. ROS act as second messengers in intracellular signaling cascades;[79] therefore, excess ROS production may play a crucial role in the modulation of gene expression, thus leading to inflammation or apoptosis under conditions of TiO_2 NP exposure. Intense up-regulation of oxidative and inflammatory pathways in mouse kidneys with TiO_2 NP-induced nephrotoxicity was compounded by severe impairment of Nrf2 expression, as demonstrated by marked reduction in nuclear content and elevation of its suppressor molecule, Keap1. As expected, impaired Nrf2 expression in the kidneys of mice with TiO_2 NP-induced chronic renal injury was associated with down-regulation of its measured target gene products including GST, HO-1, and GCLC. These enzymes protect against oxidative stress-induced cytotoxicity and tissue injury, either directly by neutralizing ROS or indirectly by catalyzing production of antioxidant and detoxifying substrates. For instance, GST catalyzes the detoxification of lipid peroxides and xenobiotics by conjugating them with GSH.[65] HO-1 is a relatively novel enzyme with potent anti-inflammatory and cytoprotective antioxidant effects.[49−51,80−84] GCL is recognized as the rate-limiting enzyme in GSH biosynthesis and is a heterodimeric enzyme composed of a 72.8 kDa GCLC and 30.8 kDa regulatory modifier (GCLM) subunit, which are distinct gene products encoded by genes on different chromosomes. GCLC possesses catalytic activity, whereas GCLM imparts catalytic characteristics to the holoenzyme that are more compatible with the cellular concentrations of reactants and feedback control by GSH.[85] Our data suggest that HO-1 and GCLC expression is dramatically decreased in kidneys with increased TiO_2 NP doses, which leads to a significant reduction in GSH level. The reductions in GST, HO-1, and GCLC expression due to exposure to TiO_2 NPs may be mediated

through the Nrf2 signal transduction pathway. It has been reported that the cyclopentenone prostaglandin compound and *tert*-butylhydroquinone induce HO-1 and GCLC expression through the Nrf2 pathway in animals.[50,86−88] Inhibition of HO-1 and GCLC expression can be interpreted as a cellular defense reaction against oxidative stress. These findings show that reductions of GST, GCLC, and HO-1 expression and antioxidant capacity may be via the Nrf2/ARE signaling pathway in TiO_2 NP-induced oxidative stress and inflammation in the kidneys. Furthermore, the present findings also showed that decreased expression of Nrf2, GST, GCLC, and HO-1 was correlated with increased kidney indices, ROS production, and levels of MDA, PC 8-OHdG, and CR and decreased levels of UA and BUN. Thus, the observed impairment of the Nrf2 expression and consequent down-regulation of its antioxidant and detoxifying target gene products play a major role in the pathogenesis and progression of kidney disease in mice.

Besides increasing the vulnerability of the diseased kidney to the adverse effects of oxidative stress, inhibition of Nrf2 expression contributes to the development and amplification of intrarenal inflammation by promoting accumulation of hydroperoxides and lipoperoxides, which are potent activators of NF-κB. To investigate further oxidative and inflammatory pathways by chronic exposure to TiO_2 NPs, NF-κB, IκB, NOX4, and COX-2 expression was examined. In the current study, oxidative stress and inflammation in mouse kidneys following exposure to TiO_2 NPs were associated with significantly increased expression of NF-κB, as shown by decreased expression of its repressor molecule IκB, as well as up-regulation of COX-2 and NOX in renal tissue. It has been reported that changes in cytokine levels and ROS generated by TiO_2 NPs can contribute to NF-κB activation.[22,23,89,90] Transcription factors control the expression of various target proteins such as COX-2 and HO-1 in mice following exposure to TiO_2 NPs.[15,16,28] COX-2 is a classic proinflammatory gene induced by NF-κB, is highly expressed in inflamed tissues, and is known to occupy an important position in the regulation of pulmonary inflammation.[15,91−93] The major ROS-generating enzyme is NOX, a membrane-bound multicomponent enzyme complex that is present in phagocytes as well as nonphagocytic cells.[91] ROS produced by NOX have two major roles. First, superoxide is required for the respiratory burst that occurs in phagocytes, leading to microbial killing. The second role is associated with regulation of cell signaling.[94] ROS derived from NOX can specifically and reversibly react with proteins, altering their activity, localization, and half-life.[95] Several studies have also demonstrated the anti-inflammatory function of Nrf2 in mice under TiO_2 NP-induced toxicity.[15,28] The precise mechanism responsible for the decreased renal tissue Nrf2 expression in mouse kidneys caused by TiO_2 NP exposure is presently unclear. It should be noted that impaired Nrf2 activity has been demonstrated in several chronic inflammatory disorders such as chronic granulomatous disease and asthma.[96] This is due to the interference of NF-κB with the dissociation of Nrf2 from Keap1 and binding of Nrf2 to the AREs of the target genes.[97,98] Thus, the decrease in the physiological expression of Nrf2 despite the prevailing oxidative stress in the injured kidneys appears to be at least, in part, due to the accompanying renal inflammation.

In conclusion, nephrotoxicity is closely associated with decreased Nrf2 expression that contributes to the pathogenesis of oxidative stress and inflammation and amplifies their damaging effects on the kidneys caused by TiO_2 NP exposure. Therefore, the application of TiO_2 NPs should be carried out cautiously, especially in humans.

AUTHOR INFORMATION

Corresponding Author

*(F.H.) E-mail: Hongfsh_cn@sina.com. Phone: +86-0512-61117563. Fax: +86-0512- 65880103.

Author Contributions

∥Suxin Gui, Bingyan Li, Xiaoyang Zhao, Lei Sheng, and Jie Hong contributed equally to this work.

Funding

This work was supported by the National Natural Science Foundation of China (Grants 81273036 and 30901218), a project funded by the Priority Academic Program Development of Jiangsu Higher Education Institutions.

Notes

The authors declare no competing financial interest.

REFERENCES

(1) Powell, J. J.; Faria, N.; Thomas-McKay, E.; Pele, L. C. Origin and fate of dietary nanoparticles and microparticles in the gastrointestinal tract. *J. Autoimmun.* **2010**, *34*, 226−233.

(2) Skocaj, M.; Filipic, M.; Petkovic, J.; Novak, S. Titanium dioxide in our everyday life; is it safe? *Radiol. Oncol.* **2011**, *45*, 227−247.

(3) Weir, A.; Westerhoff, P.; Fabricius, L.; Hristovski, K.; von Goetz, N. Titanium dioxide nanoparticles in food and personal care products. *Environ. Sci. Technol.* **2012**, *46*, 2242−2250.

(4) Oberdörster, G.; Oberdörster, E.; Oberdörster, J. Nanotoxicology: an emerging discipline evolving from studies of ultrafine particles. *Environ. Health Perspect.* **2005**, *113* (7), 823−839.

(5) Wang, J. J.; Sanderson, B. J. S.; Wang, H. Cyto- and genotoxicity of ultrafine TiO_2 particles in cultured human lymphoblastoid cells. *Mutat. Res.* **2007**, *628*, 99−106.

(6) Warheit, D. B.; Webb, T. R.; Reed, K. L.; Frerichs, S.; Sayes, C. M. Pulmonary toxicity study in rats with three forms of ultrafine-TiO_2 particles: differential responses related to surface properties. *Toxicity* **2007**, *230*, 90−104.

(7) Li, J. G.; Li, Q. N.; Xu, G. Y.; Li, J.; Cai, X. Q.; Liu, R. L. Comparative study on the acute pulmonary toxicity induced by 3 and 20 nm TiO_2 primary particles in mice. *Environ. Toxicol. Pharmacol.* **2007**, *24*, 239−244.

(8) Wang, H. H.; Wick, R. L.; Xing, B. S. Toxicity of nanoparticulate and bulk ZnO, Al_2O_3 and TiO_2 to the nematode *Caenorhabditis elegans*. *Environ. Pollut.* **2009**, *157*, 1171−1177.

(9) Xiong, D.; Fang, T.; Yu, L.; Sima, X.; Zhu, W. Effects of nano-scale TiO_2, ZnO and their bulk counterparts on zebrafish: acute toxicity, oxidative stress and oxidative damage. *Sci. Total Environ.* **2011**, *409* (8), 1444−1452.

(10) Linkov, I.; Satterstrom, F. K.; Corey, L. M. Nanotoxicology and nanomedicine: making hard decisions. *Nanomedicine* **2008**, *4*, 167−171.

(11) Elsaesser, A.; Howard, C. V. Toxicology of nanoparticles. *Adv. Drug Delivery Rev.* **2012**, *64*, 129−137.

(12) IARC. *Carbon Black, Titanium Dioxide and Talc*; IARC Monographs on the Evaluation of Carcinogenic Risks to Humans 93; International Agency for Research on Cancer: Lyon, France, 2006.

(13) Hana, S. G.; Newsomea, B.; Hennig, B. Titanium dioxide nanoparticles increase inflammatory responses in vascular endothelial cells. *Toxicology* **2013**, *306*, 1−8.

(14) Afaq, F.; Abidi, P.; Matin, R.; Rahman, Q. Cytotoxicity, pro-oxidant effects and antioxidant depletion in rat lung alveolar macrophages exposed to ultrafine titanium dioxide. *J. Appl. Toxicol.* **1998**, *18*, 307−312.

(15) Sun, Q. Q.; Tan, D. L.; Ze, Y. G.; Sang, X. Z.; Liu, X. R.; Gui, S. X.; Cheng, Z.; Cheng, J.; Hu, R. P.; Gao, G. D.; Liu, G.; Zhu, M.; Zhao, X. Y.; Sheng, L.; Wang, L.; Tang, M.; Hong, F. S.

Pulmotoxicological effects caused by long-term titanium dioxide nanoparticles exposure in mice. *J. Hazard. Mater.* **2012**, *235*−*236*, 47−53.

(16) Sun, Q. Q.; Tan, D. L.; Zhou, Q. P.; Liu, X. R.; Cheng, Z.; Liu, G.; Zhu, M.; Sang, X. Z.; Gui, S. X.; Cheng, J.; Hu, R. P.; Tang, M.; Hong, F. S. Oxidative damage of lung and its protective mechanism in mice caused by long-term exposure to titanium dioxide nanoparticles. *J. Biomed. Mater. Res. Part A* **2012**, *100A* (10), 2554−2562.

(17) Li, B.; Ze, Y. G.; Su, Q. Q.; Zhang, T.; Sang, X. Z.; Cui, Y. L.; Wang, X. C.; Gui, S. X.; Tan, D. L.; Zhu, M.; Zhao, X. Y.; Sheng, L.; Wang, L.; Hong, F. S.; Tang, M. Molecular mechanisms of nanosized titanium dioxide-induced pulmonary injury in mice. *PLoS One* **2013**, *8* (2), e55563.

(18) Federici, G.; Shaw, B. J.; Handy, R. D. Toxicity of titanium dioxide nanoparticles to rainbow trout (*Oncorhynchus mykiss*): gill injury, oxidative stress, and other physiological effects. *Aquat. Toxicol.* **2007**, *84*, 415−430.

(19) Wang, J. X.; Zhou, G. Q.; Chen, C. Y.; Yu, H. W.; Wang, T. C.; Ma, Y. M.; Jia, G.; Gao, Y. X.; Li, B.; Sun, J.; Li, Y. F.; Jia, F.; Zhao, Y. L.; Chai, Z. F. Acute toxicity and biodistribution of different sized titanium dioxide particles in mice after oral administration. *Toxicol. Lett.* **2007**, *168*, 176−185.

(20) Ma, L.; Zhao, J. F.; Wang, J.; Duan, Y. M.; Liu, J.; Li, N.; Liu, H. T.; Yan, J. Y.; Ruan, J.; Hong, F. S. The acute liver injury in mice caused by nano-anatase TiO_2. *Nanosacle Res. Lett.* **2009**, *4*, 1275−1285.

(21) Duan, Y. M.; Liu, J.; Ma, L. L.; Li, N.; Liu, H. T.; Wang, J.; Zheng, L.; Liu, C.; Wang, X. F.; Zhang, X. G.; Yan, J. Y.; Wang, H.; Hong, F. S. Toxicological characteristics of nanoparticulate anatase titanium dioxide in mice. *Biomaterials* **2010**, *31*, 894−899.

(22) Cui, Y. L.; Gong, X. L.; Duan, Y. M.; Li, N.; Hu, R. P.; Liu, H. T.; Hong, M. M.; Zhou, M.; Wang, L.; Wang, H.; Hong, F. S. Hepatocyte apoptosis and its molecular mechanisms in mice caused by titanium dioxide nanoparticles. *J. Hazard. Mater.* **2010**, *183*, 874−880.

(23) Cui, Y. L.; Liu, H. T.; Zhou, M.; Duan, Y. M.; Li, N.; Gong, X. L.; Hu, R. P.; Hong, M. M.; Hong, F. S. Signaling pathway of inflammatory responses in the mouse liver caused by TiO_2 nanoparticules. *J. Biomed. Mater. Res. Part A* **2011**, *96* (1), 221−229.

(24) Cui, Y. L.; Liu, H. T.; Ze, Y. G.; Zhang, Z. L.; Hu, Y. Y.; Cheng, Z.; Cheng, J.; Hu, R. P.; Gao, G. D.; Wang, L.; Tang, M.; Hong, F. S. Gene expression in liver injury caused by long-term exposure to titanium dioxide nanoparticles in mice. *Toxicol. Sci.* **2012**, *128* (1), 171−185.

(25) Li, N.; Ma, L. L.; Wang, J.; Liu, J.; Duan, Y. M.; Liu, H. T.; Zhao, X. Y.; Wang, S. S.; Wang, H.; Hong, F. S. Interaction between nano-anatase TiO_2 and liver DNA from mice in vivo. *Nanoscale Res. Lett.* **2010**, *5*, 108−115.

(26) Liu, H. T.; Ma, L. L.; Liu, J.; Zhao, J. F.; Yan, J. Y.; Hong, F. S. Toxicity of nano-anatase TiO_2 to mice: liver injury, oxidative stress. *Toxicol. Environ. Chem.* **2010**, *92*, 175−186.

(27) Li, N.; Duan, Y. M.; Hong, M. M.; Zheng, L.; Fei, M.; Zhao, X. Y.; Wang, Y.; Cui, Y. L.; Liu, H. T.; Cai, J. W.; Gong, S. J.; Wang, H.; Hong, F. S. Spleen injury and apoptotic pathway in mice caused by titanium dioxide nanoparticles. *Toxicol. Lett.* **2010**, *195*, 161−168.

(28) Wang, J.; Li, N.; Zheng, L.; Wang, Y.; Duan, Y. M.; Wang, S. S.; Zhao, X. Y.; Cui, Y. L.; Zhou, M.; Cai, J. W.; Gong, S. J.; Wang, H.; Hong, F. S. P38-Nrf-2 signaling pathway of oxidative stress in mice caused by nanoparticulate TiO_2. *Biol. Trace Elem. Res.* **2011**, *140*, 186−197.

(29) Sang, X. Z.; Zheng, L.; Sun, Q. Q.; Li, N.; Cui, Y. L.; Hu, R. P.; Gao, G. D.; Cheng, Z.; Cheng, J.; Gui, S. X.; Liu, H. T.; Zhang, Z. L.; Hong, F. S. The chronic spleen injury of mice following long-term exposure to titanium dioxide nanoparticles. *J. Biomed. Mater. Res. Part A* **2012**, *100A* (4), 894−902.

(30) Sang, X. Z.; Li, B.; Ze, Y. G.; Hong, J.; Ze, X.; Gui, S. X.; Sun, Q. Q.; Liu, H. T.; Zhao, X. Y.; Sheng, L.; Liu, D.; Yu, X. H.; Hong, F. S. Toxicological effects of nanosized titanium dioxide-induced spleen injury in mice. *J. Agric. Food Chem.* **2013**, *61* (23), 5590−5599.

(31) Yu, Y.; Ren, W.; Ren, B. Nanosize titanium dioxide cause neuronal apoptosis: a potential linkage between nanoparticle exposure and neural disorder. *Neurol. Res.* **2008**, DOI: 10.1179/17431 3208X305391.

(32) Wu, J.; Liu, W.; Xue, C. B.; Zhou, S. C.; Lan, F. L.; Bi, L. Toxicity and penetration of TiO_2 nanoparticles in hairless mice and porcine skin after subchronic dermal exposure. *Toxicol. Lett.* **2009**, *191*, 1−8.

(33) Ma, L. L.; Liu, J.; Li, N.; Wang, J.; Duan, Y. M.; Yan, J. Y.; Liu, H. T.; Wang, H.; Hong, F. S. Oxidative stress in the brain of mice caused by translocated nanoparticulate TiO_2 delivered to the abdominal cavity. *Biomaterials* **2010**, *31*, 99−105.

(34) Hu, R. P.; Gong, X. L.; Duan, Y. M.; Li, N.; Che, Y.; Cui, Y. L.; Zhou, M.; Liu, C.; Wang, H.; Hong, F. S. Neurotoxicological effects and the impairment of spatial recognition memory in mice caused by exposure to TiO_2 nanoparticles. *Biomaterials* **2010**, *31*, 8043−8050.

(35) Hu, R. P.; Zheng, L.; Zhang, T.; Cui, Y. L.; Gao, G. D.; Cheng, Z.; Chen, J.; Tang, M.; Hong, F. S. Molecular mechanism of hippocampal apoptosis of mice following exposure to titanium dioxide nanoparticles. *J. Hazard. Mater.* **2011**, *191*, 32−40.

(36) Shin, J. A.; Lee, E. J.; Seo, S. M.; Kim, H. S.; Kang, J. L.; Park, E. M. Nanosized titanium dioxide enhanced inflammatory responses in the septic brain of mouse. *Neuroscience* **2010**, *165*, 445−454.

(37) Ze, Y. G.; Zheng, L.; Zhao, X. Y.; Gui, S. X.; Sang, X. Z.; Su, J. J.; Guan, N.; Zhu, L. Y.; Sheng, L.; Hu, R. P.; Cheng, J.; Cheng, Z.; Sun, Q. Q.; Wang, L.; Hong, F. S. Molecular mechanism of titanium dioxide nanoparticles-induced oxidative injury in the brain of mice. *Chemosphere* **2013**, *92*, 1183−1189.

(38) Ze, Y. G.; Hu, R. P.; Wang, X. C.; Sang, X. Z.; Ze, X.; Li, B.; Su, J. J.; Wang, Y.; Guan, N.; Zhao, X. Y.; Gui, S. X.; Zhu, L. Y.; Cheng, Z.; Cheng, J.; Sheng, L.; Sun, Q. Q.; Wang, L.; Hong, F. S. Neurotoxicity and gene-expressed profile in brain injured mice caused by exposure to titanium dioxide nanoparticles. *J. Biomed. Mater. Res. Part A* **2013**, DOI: 10.1002/jbm.a.34705.

(39) Gao, G. D.; Ze, Y. G.; Li, B.; Zhao, X. Y.; Zhang, T.; Sheng, L.; Hu, R. P.; Gui, S. X.; Sang, X. Z.; Sun, Q. Q.; Cheng, J.; Cheng, Z.; Wang, L.; Tang, M.; Hong, F. S. Ovarian dysfunction and gene-expressed characteristics of female mice caused by long-term exposure to titanium dioxide nanoparticles. *J. Hazard. Mater.* **2012**, *243*, 19−27.

(40) Zhao, X. Y.; Ze, Y. G.; Gao, G. D.; Sang, X. Z.; Li, B.; Gui, S. X.; Sheng, L.; Sun, Q. Q.; Cheng, J.; Cheng, Z.; Hu, R. P.; Wang, L.; Hong, F. S. Nanosized TiO_2-induced reproductive system dysfunction and its mechanism in female mice. *PLoS One* **2013**, *8* (4), e59378.

(41) Sheng, L.; Wang, X. C.; Sang, X. Z.; Ze, Y. G.; Zhao, X. Y.; Liu, D.; Gui, S. X.; Sun, Q. Q.; Cheng, J.; Cheng, Z.; Hu, R. P.; Wang, L.; Hong, F. S. Cardiac oxidative damage in mice following exposure to nanoparticlate titanium dioxide. *J. Biomed. Mater. Res. Part A* **2013**, DOI: 10.1002/jbm.a.34634.

(42) Scown, T. M.; van Aerle, R. Y.; Johnston, B. D.; Cumberland, S.; Lead, J. R.; Richard, O.; Tyler, C. R. High doses of intravenously administered titanium dioxide nanoparticles accumulate in the kidneys of rainbow trout but with no observable impairment of renal function. *Toxicol. Sci.* **2009**, *109*, 372−380.

(43) Chen, J. Y.; Dong, X.; Zhao, J.; Tang, G. P. In vivo acute toxicity of titanium dioxide nanoparticles to mice after intraperitoneal injection. *J. Appl. Toxicol.* **2009**, *29*, 330−337.

(44) Liu, H. T.; Ma, L. L.; Zhao, J. F.; Liu, J.; Yan, J. Y.; Ruan, J.; Hong, F. S. Biochemical toxicity of mice caused by nano-anatase TiO_2 particles. *Biol. Trace Elem. Res.* **2009**, *129*, 170−180.

(45) Zhao, J. F.; Wang, J.; Wang, S. S.; Zhao, X. Y.; Yan, J. Y.; Ruan, J.; Li, N.; Duan, Y. M.; Wang, H.; Hong, F. S. The mechanism of oxidative damage in nephrotoxicity of mice caused by nano-anatase TiO_2. *J. Exp. Nanosci.* **2010**, *5* (5), 447−462.

(46) Gui, S. X.; Zhang, Z. L.; Zheng, L.; Sun, Q. Q.; Sang, X. Z.; Liu, X. R.; Gao, G. D.; Cui, Y. L.; Cheng, Z.; Cheng, J.; Tang, M.; Hong, F. S. The molecular mechanism of kidney injury of mice caused by exposure to titanium dioxide nanoparticles. *J. Hazard. Mater.* **2011**, *195*, 365−370.

(47) Gui, S. X.; Sang, X. Z.; Zheng, L.; Ze, Y. G.; Zhao, X. Y.; Sheng, L.; Sun, Q. Q.; Cheng, Z.; Cheng, J.; Hu, R. P.; Wang, L.; Hong, F. S.; Tang, M. Intragastric exposure to titanium dioxide nanoparticles

induced nephrotoxicity in mice, assessed by physiological and gene expression modifications. *Particle Fibre Toxicol.* **2013**, *10*, 4.
(48) Li, W.; Khor, T. O.; Xu, C.; Shen, G.; Jeong, W. S.; Yu, S.; Kong, A. N. Activation of Nrf2-antioxidant signaling attenuates NF-κB-inflammatory response and elicits apoptosis. *Biochem. Pharmacol.* **2008**, *76*, 1485−1489.
(49) Sen, C. K.; Packer, L. Antioxidant and redox regulation of gene transcription. *FASEB J.* **1996**, *10*, 709−720.
(50) Yang, H.; Magilnick, N.; Lee, C.; Kalmaz, D.; Ou, X.; Chan, J.; Lu, S. Nrf1 and Nrf2 regulate rat glutamate-cysteine ligase catalytic subunit transcription indirectly via NF-κB and AP-1. *Mol. Cell. Biol.* **2005**, *25*, 5933−5946.
(51) Maines, M. D. Heme oxygenase: function, multiplicity, regulatory mechanism, and clinical applications. *FASEB J.* **1988**, *2*, 2557−2568.
(52) Cantoni, L.; Rossi, C.; Rizzardini, M.; Gardina, M.; Ghezzi, P. Interleukin-1 and tumor necrosis factor induce hepatic haeme oxygenase. *Biochem. J.* **1991**, *279*, 891−894.
(53) Okinaga, S.; Takahashi, K.; Takeda, K.; Yoshizawa, M.; Fujita, H.; Sasaki, H.; Shibahara, S. Regulation of human heme oxygenase-1 gene expression under thermal stress. *Blood* **1996**, *87*, 5074−5084.
(54) Maines, M. D. The heme oxygenase system: a regulator of second messenger gases. *Annu. Rev. Pharmacol. Toxicol.* **1997**, *37*, 517−554.
(55) Willis, D.; Moore, A. R.; Frederick, R.; Willoughby, D. A. Heme oxygenase: a novel target for the modulation of the inflammatory response. *Nat. Med.* **1996**, *2*, 87−90.
(56) Chen, K.; Gunter, K.; Maines, M. D. Neurons overexpressing heme oxygenase-1 resist oxidative stress-mediated cell death. *J. Neurochem.* **2002**, *75* (1), 304−313.
(57) Okouchi, M.; Okayama, N.; Alexander, J. S.; Aw, T. Y. Nrf2-dependent glutamate-L-cysteine ligase catalytic subunit expression mediates insulin protection against hyperglycemia-induced brain endothelial cell apoptosis. *Curr. Neurovasc. Res.* **2006**, *3*, 249−261.
(58) Itoh, K.; Chiba, T.; Takahashi, S.; Ishii, T.; Igarashi, K.; Katoh, Y.; Oyake, T.; Hayashi, N.; Satoh, K.; Hatayama, I.; Yamamoto, M.; Nabeshima, Y. An Nrf2/small Maf heterodimer mediates the induction of phase II detoxifying enzyme genes through antioxidant response elements. *Biochem. Biophys. Res. Commun.* **1997**, *236*, 313−322.
(59) Yachie, A.; Niida, Y.; Wada, T.; Igarashi, N.; Kaneda, H.; Toma, T.; Ohta, K.; Kasahara, Y.; Koizumi, S. Oxidative stress causes enhanced endothelial cell injury in human heme oxygenase-1 deficiency. *Clin. Invest.* **1999**, *103* (1), 129−135.
(60) Chan, K.; Han, X. D.; Kan, Y. W. An important function of Nrf2 in combating oxidative stress: detoxification of acetaminophen. *Proc. Natl. Acad. Sci. U.S.A.* **2001**, *98*, 4611−4616.
(61) Kim, Y. C.; Masutani, H.; Yamaguchi, Y.; Itoh, K.; Yamamoto, M.; Yodoi, J. Hemin induced activation of the thioredoxin gene by Nrf2. A differential regulation of the antioxidant responsive element by a switch of its binding factors. *J. Biol. Chem.* **2010**, *276*, 18399−18406.
(62) Kostaropoulos, I.; Papadopoulos, A. I.; Metaxakis, A.; Boukouvala, E.; Papadopoulou-Mourkidou, E. Glutathione *S*-transferase in the defence against pyrethroids in insects. *Insect Biochem. Mol. Biol.* **2001**, *31*, 313−319.
(63) Hemingway, J.; Hawkes, N. J.; McCarroll, L.; Ranson, H. The molecular basis of insecticide resistance in mosquitoes. *Insect Biochem. Mol. Biol.* **2004**, *34*, 653−665.
(64) Hurst, R.; Bao, Y.; Jemth, P.; Mannervik, B.; Williamson, G. Phospholipid hydroperoxide glutathione peroxidase activity of human glutathione transferases. *Biochem. J.* **1998**, *332*, 97−100.
(65) Sivori, J. L.; Casabe, N.; Zerba, E. N.; Wood, E. J. Induction of glutathione *S*-transferase activity in *Triatoma infestans*. *Mem. Inst. Oswaldo Cruz* **1997**, *92*, 797−802.
(66) Yang, P.; Lu, C.; Hua, N.; Du, Y. Titanium dioxide nanoparticles co-doped with Fe^{3+} and Eu^{3+} ions for photocatalysis. *Mater. Lett.* **2002**, *57*, 794−801.
(67) Oliveira, C. P.; Lopasso, F. P.; Laurindo, F. R.; Leitao, R. M.; Laudanna, A. A. Protection against liver ischemia-reperfusion injury in rats by silymarin or verapamil. *Transplant. Proc.* **2001**, *33*, 3010−3014.
(68) Nourooz-Zadeh, J.; Tajaddini-Sarmadi, J.; Wolff, S. P. Measurement of plasma hydroperoxide concentrations by the ferrous oxidation-xylenol orange assay in conjunction with triphenylphosphine. *Anal. Biochem.* **1994**, *220*, 403−409.
(69) Buege, J. A.; Aust, S. D. Microsomal lipid peroxidation. *Methods Enzymol.* **1978**, *52*, 302−310.
(70) Fagan, J. M.; Bogdan, G. S.; Sohar, I. Quantitation of oxidative damage to tissue proteins. *Int. J. Biochem. Cell Biol.* **1999**, *31*, 751−757.
(71) Hissin, P. J.; Hilf, R. A. Fluorometric method for determination of oxidized and reduced glutathione in tissues. *Anal. Biochem.* **1976**, *74*, 214−226.
(72) Ke, L. D.; Chen, Z.; Yung, W. K. A. A reliability test of standard-based quantitative PCR: exogenous vs endogenous standards. *Mol. Cell Probes* **2000**, *14*, 127−135.
(73) Livak, K. J.; Schmittgen, T. D. Analysis of relative gene expression data using real-time quantitative PCR and the 2(T) (−ΔΔC) method. *Methods* **2001**, *25*, 402−408.
(74) Liu, W. H.; Saint, D. A. Validation of a quantitative method for real time PCR kinetics. *Biochem. Biophys. Res. Commun.* **2002**, *294*, 347−353.
(75) Benani, A.; Troy, S.; Carmona, M. C.; Fioramonti, X.; Lorsignol, A.; Leloup, C.; Casteilla, L.; Pénicaud, L. Role for mitochondrial reactive oxygen species in brain lipid sensing: redox regulation of food intake. *Diabetes* **2007**, *56*, 152−160.
(76) Wolfgang, M. J.; Cha, S. H.; Sidhaye, A.; Chohnan, S.; Cline, G.; Shulman, G. I.; Lane, M. D. Regulation of hypothalamic malonyl-CoA by central glucose and leptin. *Proc. Natl. Acad. Sci. U.S.A.* **2007**, *104*, 19285−19290.
(77) Leloup, C.; Magnan, C.; Benani, A.; Bonnet, E.; Alquier, T.; Offer, G.; Carriere, A.; Périquet, A.; Fernandez, Y.; Ktorza, A.; Casteilla, L.; Pénicaud, L. Mitochondrial reactive oxygen species are required for hypothalamic glucose sensing. *Diabetes* **2006**, *55*, 2084−2090.
(78) Sardari, R. R. R.; Zarchi, S. R.; Talebi, A.; Nasri, S.; Imani, S.; Khoradmehr, A.; Sheshde, S. A. R. Toxicological effects of silver nanoparticles in rats. *Afr. J. Microbiol. Res.* **2012**, *6* (27), 5587−5593.
(79) Valko, M.; Rhodes, C. J.; Moncol, J.; Izakovic, M.; Mazur, M. Free radicals, metals and antioxidants in oxidative stress-induced cancer. *Chem. Biol. Interact.* **2006**, *160*, 1−40.
(80) Yoh, K.; Itoh, K.; Enamoto, A.; Hirayama, A.; Yamaguchi, N.; Kobayashi, M.; Morito, N.; Koyama, A.; Yamamoto, M.; Takahashi, S. Nrf2-deficient female mice develop lupus-like autoimmune nephritis. *Kidney Int.* **2001**, *50*, 1343−1353.
(81) Yoh, K.; Hirayama, A.; Ishizaki, K.; Yamada, A.; Takeuchi, M.; Yamagishi, S.; Morito, N.; Nakano, T.; Ojima, M.; Shimohata, H.; Itoh, K.; Takahashi, S.; Yamamoto, M. Hyperglycemia induces oxidative and nitrosative stress and increases renal functional impairment in Nrf2-deficient mice. *Genes Cells* **2008**, *13*, 1159−1170.
(82) Morse, D.; Choi, A. M. Heme oxygenase-1: the "emerging molecule" has arrived. *Am. J. Respir. Cell Mol. Biol.* **2002**, *27*, 8−16.
(83) Otterbein, L. E.; Soares, M. P.; Yamashita, K.; Bach, F. H. Heme oxygenase-1: unleashing the protective properties of heme. *Trends Immunol.* **2003**, *24*, 449−455.
(84) Chen, C. Y.; Jang, J. H.; Li, M. H.; Surh, Y. J. Resveratrol upregulates heme oxygenase-1 expression via activation of NF-E2-related factor 2 in PC12 cells. *Biochem. Biophys. Res. Commun.* **2005**, *331*, 993−1000.
(85) Griffith, O. W.; Mulcahy, R. T. The enzymes of glutathione synthesis:γ-glutamylcysteine synthetase. *Adv. Enzymol. Relat. Areas Mol. Biol.* **1999**, *73*, 209−267.
(86) Lee, J. S.; Surh, Y. J. Nrf2 as a novel molecular target for chemoprevention. *Cancer Lett.* **2005**, *224*, 171−184.
(87) Lim, H. J.; Lee, K. S.; Lee, S.; Park, J. H.; Choi, H. E.; Go, S. H.; Kwak, H. J.; Park, H. Y. 15d-PGJ2 stimulates HO-1 expression through p38 MAP kinase and Nrf-2 pathway in rat vascular smooth muscle cells. *Toxicol. Appl. Pharmacol.* **2007**, *223*, 20−27.
(88) Itoh, K.; Wakabayashi, N.; Katoh, Y.; Ishii, T.; O'connor, T.; Yamamoto, M. Keap1 regulates both cytoplasmic-nuclear shuttling and

degradation of Nrf2 in response to electrophiles. *Genes Cells* **2003**, *8*, 379−391.
(89) Hayden, M. S.; Ghosh, S. Shared principles in NF-κB signaling. *Cell* **2008**, *132*, 344−362.
(90) Karin, M.; Yamamoto, Y.; Wang, Q. M. The IKK NF-κB system: a treasure trove for drug development. *Nat. Rev. Drug Discov.* **2004**, *3*, 17−26.
(91) Smith, W. L.; Michael Garavito, R.; DeWit, D. L. Prostaglandin endoperoxide H syntheses (cyclooxygenases)-1 and -2. *J. Biol. Chem.* **1996**, *271* (52), 33157−33160.
(92) Tanabe, T.; Tohnai, N. Cyclooxygenase isozymes and their gene structures and expression. *Prostaglandins Other Lipid Mediat.* **2002**, *68*−*69*, 95−114.
(93) Park, G. Y.; Christman, J. W. Involvement of cyclooxygenase-2 and prostaglandins in the molecular pathogenesis of inflammatory lung diseases. *Am. J. Physiol. Lung Cell Mol. Physiol.* **2006**, *290*, L797−L805.
(94) Rahman, I.; Biswas, S. K.; Kode, A. Oxidant and antioxidant balance in the airways and airway diseases. *Eur. J. Pharmacol.* **2006**, *533* (1−3), 222−239.
(95) Leeand, I. T.; Yang, C. M. Role of NADPH oxidase/ROSin pro-inflammatory mediators-induced airway and pulmonary diseases. *Biochem. Pharmacol.* **2012**, *84* (5), 581−590.
(96) Rieber, N.; Hector, A.; Kuijpers, T.; Roos, D.; Hartl, D. Current concepts of hyperinflammation in chronic granulomatous disease. *Clin. Dev. Immunol.* **2012**, *2012*, 252460.
(97) Dworski, R.; Han, W.; Blackwell, T. S.; Hoskins, A.; Freeman, M. L. Vitamin E prevents Nrf2 suppression by allergens in asthmatic alveolar macrophages in vivo. *Free Radical Biol. Med.* **2011**, *51*, 516−521.
(98) Yu, M.; Li, H.; Liu, Q.; Liu, F.; Tang, L.; Li, C.; Yuan, Y.; Zhan, Y.; Xu, W.; Li, W.; Chen, H.; Ge, C.; Wang, J.; Yang, X. Nuclear factor p65 interacts with Keap1 to repress the Nrf2-ARE pathway. *Cell Signal* **2011**, *23*, 883−892.